CHEMBIOCHEM

DOI: 10.1002/cbic.200900011

Insights into Sequence–Activity Relationships amongst Baeyer–Villiger Monooxygenases as Revealed by the Intragenomic Complement of Enzymes from *Rhodococcus jostii* RHA1

Claudia Szolkowy,[a] Lindsay D. Eltis,[b] Neil C. Bruce,[c] and Gideon Grogan*[a]

Microbial genome sequences are providing a wealth of information on new enzymes that have considerable potential as biocatalysts. The recently sequenced genome of *Rhodococcus jostii* RHA1, for example, has revealed an impressive array of catabolic enzymes, including many putative Baeyer–Villiger monooxygenases (BVMOs). We have cloned 23 target BVMO sequences from the genome of *R. jostii* RHA1 and heterologously expressed 13 of these as soluble proteins to unearth new substrate specificities and selectivities. Whole-cell biocatalysts expressing the genes were screened against seven different test substrates. Each of these catalysts displayed activity toward at least three ketones. We observed a remarkable diversity of both regio- and enantioselectivity among the BVMOs from *R. jostii* RHA1 for the transformation of two chiral substrates, with some enzymes displaying high enantioselectivity for the isomers of 2-methylcyclopentanone. With the notable exception of the product of gene *ro03437*, named MO14, the biocatalysts' sequences correlated well with their respective activities and selectivities. This correlation allowed the identification of sequence motifs specific to subgroups of the BVMOs from *R. jostii* and other organisms. Overall, the data improve predictive models of BVMO activity from sequence and suggest new avenues to pursue in engineering these enzymes.

Introduction

Baeyer–Villiger monooxygenases (BVMOs; E.C. 1.4.13.22), typified by the cyclohexanone monooxygenase from *Acinetobacter calcoaceticus* NCIMB 9871 ($CHMO_{9871}$)[1] catalyse the insertion of oxygen into carbon skeletons adjacent to carbonyl groups. This reaction is a formal biological equivalent of the chemical Baeyer–Villiger reaction, which is classically achieved by using peracids such as *meta*-chloroperbenzoic acid.[2] BVMOs have stimulated great interest as catalysts for organic synthesis as they display superior regio- and enantioselectivity compared to the organometallic catalysts currently available for chiral Baeyer–Villiger reactions.[3] BVMOs are dependent on two cofactors: a nicotinamide coenzyme (usually NADPH) and a flavin prosthetic group (usually FAD). During the catalytic cycle, NADPH is used to reduce the FAD in the active site of the enzyme. The reduced flavin, $FADH_2$, then reacts with molecular oxygen to form a peroxidate ion, which is the reactive species in the Baeyer–Villiger oxidation. The mechanism involves the formation, and subsequent rearrangement of, a tetrahedral Criegee intermediate, which is the key species in both the "chemical" and enzymatic reaction.

Since the adoption of $CHMO_{9871}$ as a model for studying the potential of these enzymes, a large range of substrates has been identified for the biological Baeyer–Villiger reaction, catalysed either by $CHMO_{9871}$ itself or a few other Baeyer–Villiger monooxygenase enzymes,[4,5] most of which have been identified through genome-mining approaches.[6] The sequences of known BVMOs are typically between 500 and 550 amino acids in length and contain two Rossman fold motifs (GXGXX(G/A)) for the binding of ADP moieties of each cofactor—one near the N terminus and the other approximately 200 amino acids from the N terminus of the enzyme. In addition, a BVMO motif (FXGXXXHXXXW(P/D)) has been described, closely upstream from the second Rossman motif, that has greatly aided in the identification of putative BVMO sequences in sequenced genomes.[7] Studies on one BVMO, 4-hydroxyacetophenone monooxygenase (HAPMO) from *Pseudomonas fluorescens* ACB, have suggested that the histidine residue in this motif is crucial for catalysis, since mutation to alanine suppressed the catalytic activity of the enzyme.[7] A related class of enzymes, flavin-containing monooxygenases (FMOs), possess a similar motif with the amino acid sequence FXGXXXHXXX(Y/F), but are more distantly related in sequence overall.[7,8] The sole X-ray crystal structure of a BVMO solved thus far, that of phenyl-

[a] *C. Szolkowy, Dr. G. Grogan*
York Structural Biology Laboratory, Department of Chemistry
University of York, York YO10 5YW (UK)
Fax: (+44) 1904-328266
E-mail: grogan@ysbl.york.ac.uk

[b] *Prof. Dr. L. D. Eltis*
Department of Microbiology and Immunology, Life Sciences Centre
University of British Columbia, 2350 Health Sciences Mall
Vancouver V6T 1Z3, BC (Canada)

[c] *Prof. Dr. N. C. Bruce*
Centre for Novel Agricultural Products, Department of Biology
University of York, York YO10 5YW (UK)

Supporting information for this article is available on the WWW under http://dx.doi.org/10.1002/cbic.200900011.

acetone monooxygenase (PAMO) from the thermophilic bacterium *Thermobifida fusca* in complex with FAD, revealed that the fingerprint motif for Baeyer–Villiger monooxygenases FXGXXXHXXXW(P/D) is found on the surface of the enzyme,[9] and it was suggested that this motif might be implicated in conformational changes of the enzyme during the catalytic cycle. The further role of conformational changes in BVMO activity has been difficult to assess, as there is as yet no structure of the enzyme that features a bound substrate or product; however, the structure has proved extremely useful in informing engineering studies of both PAMO and other BVMOs.[10–12]

Many studies of BVMOs have focused on the molecular determinants of regio- and enantioselectivity within the active site, as knowledge of these would allow rational mutation of the enzyme with a view to improving or expanding these properties. Expanding the range of BVMO activities has been achieved in three ways. First, the random mutagenesis of BVMOs such as $CHMO_{9871}$ and cyclopentanone monooxygenase from *Comamonas* sp. NCIMB 9872 (CPMO) has revealed mutants of broader substrate specificity and improved, or even inverted, enantioselectivity.[10,11] Second, the structure of PAMO has been used to target active-site residues in order to rationally engineer this enzyme for improved properties.[12] Third, there is an increasing number of catalysts appearing within the gene databases that hint at a rich reservoir of untapped activities and selectivities that have arisen as a result of natural evolutionary processes.[13] These have recently included enzymes from *Pseudomonas fluorescens* DSM 50106,[14,15] *Pseudomonas veronii* (mekA)[16] and *Pseudomonas putida* KT2440[17] that display a preference for aliphatic ketone substrates, and a CHMO homologue from *Xanthobacter* sp. ZL5 that catalyses the oxygenation of sterically demanding ketone substrates.[18,19]

The genome sequence of *R. jostii* RHA1 has proven particularly interesting in the last regard, revealing that this bacterium has an unusually large amount of putative BVMOs displaying a variety of the sequence attributes seen amongst the known enzymes as well as others that have not yet been characterised.[20] In the interests of both exploring this intragenomic diversity and highlighting the activities of potential new catalysts, we have amplified and cloned the closest 23 homologues to $CHMO_{9871}$ from *R. jostii* RHA1. Thirteen of these targets were produced as soluble proteins in *Escherichia coli*, and their activity as whole-cell biocatalysts was assessed with various ketones. Analysis of the amino acid sequence of these BVMOs, in conjunction with both their substrate spectrum and regio- and enantioselectivity data, has allowed these enzymes to be grouped as well as group-specific amino acid sequences to be identified. In addition to describing new and potentially useful activities, the studies reveal previously unrecognised relationships between the enzymes and new regions of sequence that might be targeted for rational design in the future by using these candidate enzymes as starting points.

Results

Sequences of BVMOs from *R. jostii* RHA1

Twenty-three open reading frames encoding putative Baeyer–Villiger monooxygenases from *R. jostii* RHA1 were chosen as targets for this study (Table 1). These represent the closest homologues to $CHMO_{9871}$, the sequence search model. The enzymes, designated MO1 to MO23, share 12 to 43% sequence identity with $CHMO_{9871}$. Full amino acid sequences can be found as part of a full sequence alignment in the Supporting Information. Fifteen of the targets possess the amino acid fingerprint motif FXGXXXHXXXW(P/D) that has been proposed to identify the sequences as encoding a BVMO.[7] Two of the 15 (MO21 and MO23) have identical amino acid sequences save for a substitution from Leu (MO21) to Arg (MO23) in position 480 that has resulted from a single base-pair difference. Both MO21 and MO23 have a histidine residue in place of the lysine that is found in position 336 in PAMO and which is well conserved amongst all other known BVMOs. The remaining eight targets have one or two substitutions in the fingerprint motif, such as FXGXXXHXXXWN (for example, MO2), YXGXXXHXXXWR (MO4), FXGXXXLXXXWP (MO14) and FXGXXXHXXXYD (MO22). In addition, MO22 contains the motif reported to be characteristic of FMO[7] and was included in our target selection in order to explore the possible Baeyer–Villiger monooxygenase activity of such an enzyme.

Table 1. Overview of the Baeyer–Villiger monooxygenases MO1 to MO23 from *R. jostii* RHA1 and their corresponding gene annotations.

Trivial name	Gene name	Trivial name	Gene name
MO1	ro06679	MO13	ro03773
MO2	ro04304	MO14	ro03437
MO3	ro03247	MO15	ro02492
MO4	ro03063	MO16	ro02919
MO5	ro02109	MO17	ro05228
MO6	ro01874	MO18	ro05396
MO7	ro06008	MO19	ro05522
MO8	ro08998	MO20	ro08137
MO9	ro09035	MO21	ro10187
MO10	ro09039	MO22	ro00824
MO11	ro06698	MO23	ro08185
MO12	ro07112	–	–

The 23 targeted genes were amplified by using the genomic DNA from *R. jostii* RHA1 as a template and cloned in the pET-YSBLIC-3C vector by using a LIC-PCR cloning method.[13] The integrity of each of the recombinant genes was then verified by nucleotide sequencing. Of a number of expression strains of *E. coli* assessed for soluble protein production, the most successful overall proved to be *E. coli* Rosetta 2 (DE3) pLysS, in which 12 of the CHMO homologues (MO3, MO4, MO9, MO10, MO11, MO14, MO15, MO16, MO18, MO20, MO21 and MO23) were produced as soluble proteins, including two with variant fingerprint motifs (MO4 and MO14), two "long" BVMOs with N-terminal extensions reminiscent of HAPMO[21] (MO10 and MO18) and the FMO homologue MO22.

A full sequence alignment of the target enzymes, obtained by using the programme ClustalW,[22] is shown in the Supporting Information, and partial alignments are shown at the relevant points in this report. A second alignment was generated by using a group of sequences that included the *R. jostii* RHA1 BVMOs (excluding MO22, which has only 12% sequence identity with $CHMO_{9871}$), HAPMO, PAMO, CPMO and a selection of BVMOs from different organisms ($CHMO_{Brach}$, $CHMO_{Brev1}$, $CHMO_{Brev2}$, $CHMO_{Rhodo}$, $CHMO_{Arthr}$, $CHMO_{Xantho}$, $BVMO_{mekA}$, $BVMO_{Pf}$, $BVMO_{EtaA}$, $BVMO_{Rv3049c}$ and CPDMO) that were the subject of previous sequence–activity relationship studies.[19,23] Sequences were used as input into the PROML programme of the PHYLIP package in order to generate a phylogenetic tree with an associated bootstrap analysis, based on 100 calculations (Figure 1). The initial groupings of enzymes on the tree, assigned as groups I–V for the most significant groups in this study, are useful as they allow the experimentally determined selectivities of the RHA1 enzymes to be assessed in the context of previously reported activities, notably those that have been used to classify known BVMOs on the basis of their sequence and selectivity.[19,23]

MO3, MO4, MO11 and MO20 (group I) share 44 to 57% sequence identity and cluster with CPMO and $CHMO_{Brev2}$. MO9, MO14 and MO15 (group II) share 50 to 61% sequence identity and cluster with PAMO. MO21 and MO23 (only MO21 shown), which differ by a single residue, and the $BVMO_{mekA}$ from *Pseudomonas veronii*, which displays a preference for aliphatic substrates, are intermediate between group I and II enzymes because they have approximately 40% sequence identity to both MO3 (group I) and MO9 and MO15 (group II). Most of the CHMO enzymes cluster together, as previously observed, and form group III. The N-terminally extended enzymes, MO10 and MO18 (group IV) cluster with HAPMO. MO16, in group V, is more distantly related to the other BVMOs under consideration, but clusters with the BVMO from *Mycobacterium tuberculosis* EtaA,[24] with which it shares 58% sequence identity, and with the BVMO from *Pseudomonas putida* KT2440.[17]

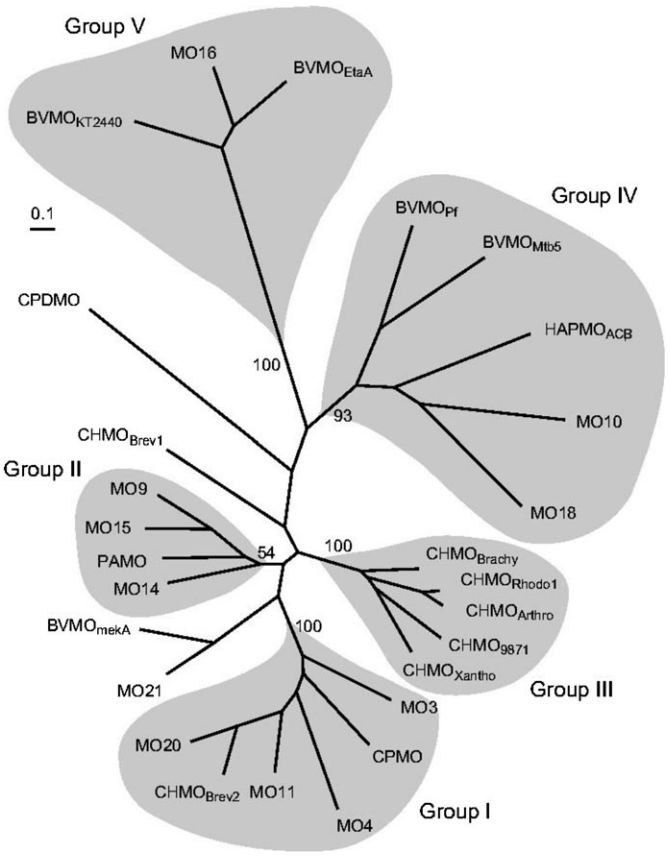

Figure 1. Radial phylogram of catalytically active BVMOs from *R. jostii* RHA1 and previously studied BVMOs. Groups I–V are shaded and labelled. Bootstrap values are given on the relevant branches of the tree. Sequences other than those of RHA1 are: $CHMO_{9871}$, cyclohexanone monooxygenase from *Acinetobacter calcoaceticus* (Uniprot ID: Q9R2F5); $CHMO_{Brev1}$ and $CHMO_{Brev2}$ from *Brevibacterium* sp. HCU (Q9F014 and Q9FDI3, respectively); $CHMO_{Arthr}$ from *Arthrobacter* sp. BP2 (Q84H88); $CHMO_{Rhodo1}$ from *Rhodococcus* sp. Phi1 (Q84H73); $CHMO_{Brach}$ from *Brachymonas petroleovorans* (Q5VJEO); $CHMO_{Xantho}$, from *Xanthobacter* sp. ZL5 (Q8VLS4); CPMO, cyclopentanone monooxygenase from *Comamonas* sp. NCIMB 9872 (Q8GAW0); $BVMO_{mekA}$ from *Pseudomonas veronii* MEK700 (Q0MRG6); $BVMO_{Pf}$ from *Pseudomonas fluorescens* DSM 50106 (O87636); HAPMOACB, 4-hydroxyacetophenone monooxygenase from *Pseudomonas fluorescens* (Q93J5); CPDMO, cyclopentadecanone monooxygenase from *Pseudomonas* sp. strain HI-70 (Q1T7B5); $BVMO_{Mtb5}$ from *Mycobacterium tuberculosis* H37Rv (O53294); $BVMO_{EtaA}$ from *Mycobacterium tuberculosis* H37Rv (P96223); $BVMO_{KT2440}$ from *Pseudomonas putida* (Q88J44).

A screen of substrate preference in *R. jostii* RHA1 BVMOs

In order to shed light on the substrate specificity of some of the rhodococcal BVMOs, an initial screen was performed in which the recombinant whole-cell biocatalysts were challenged with seven commercially available ketones (Scheme 1). *E. coli* has not been shown to possess enzymes capable of performing the Baeyer–Villiger reaction, thus substrate profiling of these enzymes in recombinant whole-cell form has been the method of choice in recent reports.[23,25,26] The seven compounds for the biotransformation screen represent three types of substrates: simple cyclic ketones (cyclobutanone (**1**), cyclopentanone (**2**), cyclohexanone (**3**) and cycloheptanone (**4**)); chiral cyclic ketones (2-methylcyclopentanone (**5**) and bicyclo-[3.2.0]hept-2-en-6-one (**6**)); and an aliphatic ketone **7**. Bicycloheptenone **6** has been used extensively as a stereochemical model for BVMO activity.[27,28] The reaction products were analysed by gas chromatography with commercially available ketones and lactones/esters as standards.

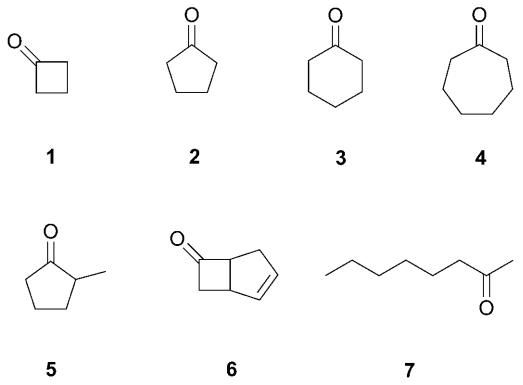

Scheme 1. Substrates used for screening the activities of *R. jostii* RHA1 BVMOs heterologously produced in *E. coli*.

Table 2. Substrate spectra of heterologously produced Baeyer–Villiger monooxygenases from *R. jostii* RHA1 in whole cells.[a]

Biocatalyst	Ketone **1**	Ketone **2**	Ketone **3**	Ketone **4**	Ketone **5**	Ketone **6**	Ketone **7**
MO3	B	A*	A*	A	A*	A	C
MO4	B	B	A	C	A*	A	C
MO9	B	C	D	D	B	B	C
MO10	C	D	D	D	C	A	D
MO11	B	B	B	B	B	B	C
MO14	B	B	C	C	B	B	C
MO15	B	C	D	D	B	B	C
MO16	B	C	C	D	B	B	B
MO18	B	C	C	C	B	A	D
MO20	B	A*	A*	A	A*	A	C
MO21	C	B	B	D	A*	A	C
MO22	B	C	D	D	B	B	D
$CHMO_{9871}$	C	C	B	B	B	B	C
pET	D	D	D	D	D	D	D

[a] $CHMO_{9871}$ was included as a positive control, and the empty pET vector, pET-YSBLIC-3C, as negative control. A* = 100% conversion, A = 56–99% conversion, B = 0–55% conversion, C = trace–9% conversion, D = no conversion.

The influence of the ring size of the cycloalkanone substrates on biocatalyst activity was then examined. In general, decreasing substrate acceptance among the biocatalysts was observed with the increasing ring size of the ketone (Figure 2), that is, cyclobutanone **1**, which is the smallest ketone, was converted by all biocatalysts. Cyclopentanone **2** was not transformed by MO10 but was transformed by the twelve other enzymes from *R. jostii* RHA1 and $CHMO_{9871}$; however, 2-methylcyclopentanone **5** was a substrate for MO10. Cyclohexanone **3** was converted by nine biocatalysts and the cycloheptanone **4** only by seven.

The results from the initial screen are shown in Table 2. Each of the thirteen biocatalysts transformed at least three of the ketones to the corresponding Baeyer–Villiger product. In each case, *E. coli* Rosetta 2 (DE3) pLysS cells transformed with vector with no insert did not produce any Baeyer–Villiger products. By contrast, the substrate spectrum obtained for this strain expressing $CHMO_{9871}$ was consistent with previous reports in the literature for this enzyme.[1,27,29,30] Conversions of ketones **2**, **3**, **4**, **5**, and **6** were observed, although no literature was found on the biotransformation of ketones **1** and **7** by $CHMO_{9871}$.

Of the newly described biocatalysts, cells expressing MO10 displayed the narrowest substrate spectrum for these substrates, converting only the 4-membered-ring system **6** efficiently. Catalysts with the broadest substrate spectrum in this study were those expressing group I enzymes (MO3, MO4, MO11 and MO20) and MO14, which converted each of the test substrates into the corresponding Baeyer–Villiger products. Strains expressing MO3 and MO20 were also the most efficient biocatalysts, being capable of completely transforming three of the test substrates. The substrate spectrum of MO23 has been omitted from Table 2 because it differs from MO21 only by a single residue and behaved identically to this biocatalyst in all assays to date.

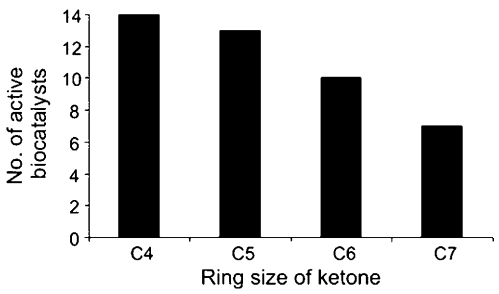

Figure 2. Bar chart illustrating the decreasing number of BVMOs active with increasing ring size of ketone substrates **1** to **4**.

It was notable that the three biocatalysts containing enzymes with the naturally variant fingerprint motifs YXGXXXHXXXWR (MO4), FXGXXXLXXXWP (MO14) and FXGXXXHXXXYD (MO22) displayed significant BVMO activity. This indicates that the previously identified fingerprint motif is not strictly conserved amongst flavoenzymes that catalyse the Baeyer–Villiger reaction. More specifically, acceptable substitutions for the highly conserved Phe, His and Pro/Asp in the fingerprint motif FXGXXXHXXXW(P/D) are Tyr, Leu and Arg, respectively.

Biotransformation screen of chiral substrates

The emerging range of BVMO biocatalysts in the literature is revealing a spectrum of enantioselectivities that have, in some instances, been correlated with the amino acid sequences of the enzymes themselves.[19,23] $CHMO_{9871}$ and other enzymes have been found to display poor enantioselectivity towards small cycloalkanones with small substituents such as **5**, although $CHMO_{9871}$ converts the same ring substituted with longer aliphatic chains with high enantioselectivity.[29] It was assumed that the methyl group in **5** is too small to engender the discrimination of (*R*)- and (*S*)-enantiomers within the active site of the enzyme.[29] Indeed, no BVMO has been reported that can effectively resolve substrate **5**. For this reason, **5** served as a simple chiral model for characterising the enantioselectivity of the rhodococcal BVMOs (Scheme 2).

A second set of experiments was performed in order to obtain information on the potential of the biocatalysts for the kinetic resolution of **5**. The enantiomeric excess of residual ketones **5** and the lactone products **8** recovered from each biotransformation was determined by chiral GC. The absolute configurations of ketones **5** and lactones **8** were assigned according to the data reported for the reaction catalysed by $CHMO_{9871}$.[29] Reactions catalysed by strains expressing MO4, MO20 and MO21 proceeded very rapidly to full conversion to

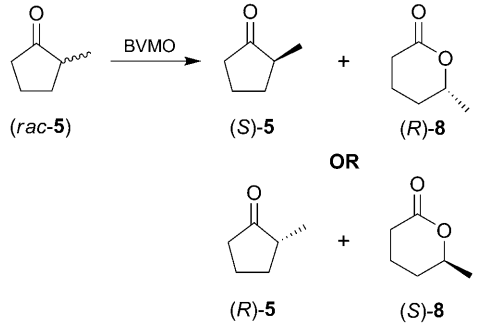

Scheme 2. Possible resolution reactions of 2-methylcyclopentanone (**5**) by BVMOs used in this study.

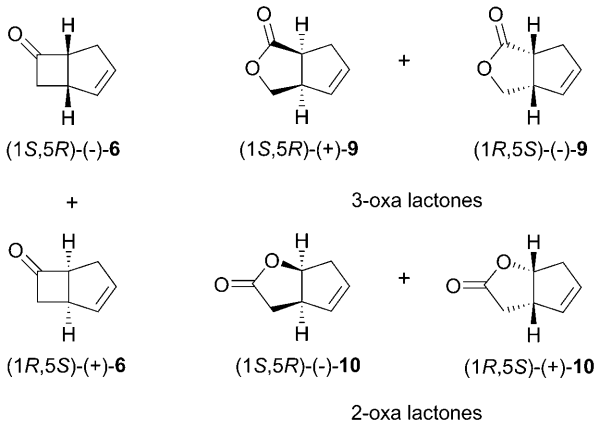

Scheme 3. Enantiomers of racemic ketone substrate **6** and lactone products **9** and **10**.

the racemic lactone product (Table 3); this is suggestive of very poor enantioselectivity in the transformation of **5**. Strains expressing biocatalysts MO9, MO15, MO18 and MO22 transformed **5** with higher enantioselectivity than the $CHMO_{9871}$ construct. To the best of our knowledge, the enantioselectivity displayed by MO18 is the best reported to date for a BVMO with this substrate,[29,31] yielding lactone (*S*)-**8** with 89% enantiomeric excess and an *E* value of 25. Enantiocomplementary partial resolutions were performed by MO9 and MO15 (*R*-selective, $E=5$) and MO22 (*S*-selective, $E=6$). Most of the other rhodococcal enzymes transformed ketone **5** with little or no enantioselectivity.

Bicyclic ketone **6** is a more complex chiral substrate, possessing two stereocentres (Scheme 3). This substrate was included in the initial screen because it is a valuable model for examining the selectivity of BVMOs, giving rise to a range of possible regio- plus stereochemical outcomes. Depending on the enzyme, racemic **6** can be classically resolved to yield enantioenriched ketone and one or more lactone products. The latter can have the oxygen inserted into either the chemically favoured 2-oxa position (giving enantiomers of lactone **10**) or the less favoured 3-oxa position (giving lactones **9**), as catalysed by both the enzymes encoded by Rv3049c from *M. tuberculosis*[13] and HAPMO.[21] Classically, BVMOs such as $CHMO_{9871}$[27] and $CHMO_{Xantho}$[18] catalyse the "enantiodivergent" biotransformation of **6** wherein each enantiomer of the racemic substrate is converted to a *different* lactone regioisomer, each with high enantiomeric excess. In a third series of experiments, each of the biocatalysts from *R. jostii* RHA1 was challenged with ketone **6**, and residual ketone substrate and lactone products were analysed by chiral GC (Figure 3).

Of the 13 rhodococcal BVMO catalysts, three (MO10, MO18 and MO21) converted the racemic ketone rapidly to nearly 100% conversion, although sufficient residual ketone remained to determine the residual substrate *ee* values by chiral GC (Table 4). Table 4 shows that, of the 13 catalysts, eight oxidised the (1*R*,5*S*)-ketone preferentially, the rest the (1*S*,5*R*)-ketone. Promising resolutions of the ketone substrate after partial conversion were observed with MO3 (59% conversion, 82% *ee* recovered ketone) and MO14 (36% conversion, 63% *ee* recovered ketone). As reported previously, $CHMO_{9871}$ appeared to transform the two enantiomers of **6** at approximately equivalent rates.[32]

Different profiles of lactone regioisomers and enantiomers were obtained when different biocatalysts were used (Figure 3). MOs 3, 4, 11, 20 (from group I), MO14 and MO22 catalysed the insertion of oxygen only at the 2-oxa position to give lactones (+)-**10** and (−)-**10**, in most cases with poor enantioselectivity (Table 5). Given the modest *ee* of the residual ketones in most cases, these transformations might best be described as regioconvergent. Of these catalysts, MO4 stood out as the only one that

Table 3. Results of the whole-cell biotransformations screen with ketone **5** as substrate.

Biocatalyst	Conversion [%]	Residual ketone	*ee*[a] (**5**) [%]	Product lactone	*ee*[a] (**8**) [%]	*E*[b] (**8**)
MO3	64	(*S*)-**5**	35	(*R*)-**8**	9	1
MO4	100	–	–	racemate	0	–
MO9	15	(*S*)-**5**	21	(*R*)-**8**	63	5
MO10	trace	–	–	–	–	–
MO11	47	(*S*)-**5**	6	(*R*)-**8**	2	1
MO14	50	(*R*)-**5**	17	(*S*)-**8**	10	1
MO15	10	(*S*)-**5**	17	(*R*)-**8**	63	5
MO16	48	(*R*)-**5**	39	(*S*)-**8**	23	2
MO18	31	(*R*)-**5**	70	(*S*)-**8**	89	25
MO20	100	–	–	racemate	0	–
MO21	100	–	–	racemate	0	–
MO22	42	(*R*)-**5**	85	(*S*)-**8**	59	6
$CHMO_{9871}$	27	(*R*)-**5**	20	(*S*)-**8**	39	3

[a] The margins of error in the determinations of *ee* are of the order of 1% *ee* according to data obtained for the standard racemic compounds. [b] *E* was generally calculated from the equation in refs. [37] and [38] for the biotransformations catalysed by MO9, MO10, MO15, MO18 and MO22.

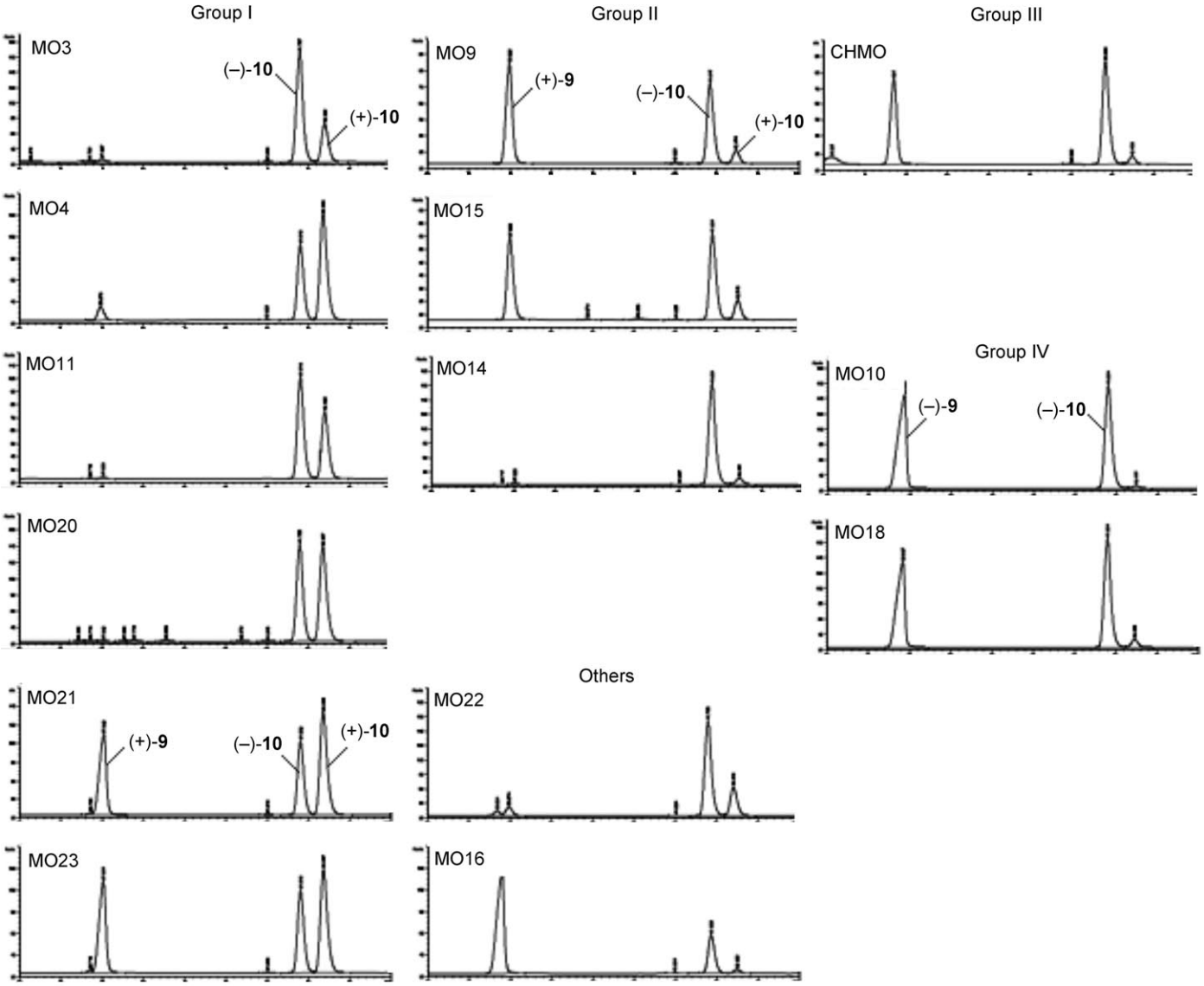

Figure 3. Chiral GC traces obtained for analysis of chiral lactones **9** and **10** synthesised by the BVMOs from *R. jostii* RHA1 and CHMO. The data obtained were used to calculate the *ee* values in Table 5.

synthesised lactone (+)-**10** in larger quantities than its enantiomeric counterpart. MO14 is also distinctive in that it appears to perform a very good resolution of the racemic ketone into one 2-oxa lactone enantiomer ((−)-**10** only), a stereochemical course that has not previously been observed for this substrate with a BVMO, and one that might be of practical utility. MO9 and MO15 (group II) were also striking, transforming a single ketone enantiomer, (+)-**6**, to the two regioisomeric lactones (+)-**9** and (−)-**10**, both in high *ee*. This is again an unprecedented stereochemical course for this reaction with a BVMO. Many enzymes synthesised a mixture of the two regioisomeric lactones **9** and **10**, with MOs 10 and 18 (group IV) and MO16 (group V) displaying the same enantiodivergent stereochemical behaviour as $CHMO_{9871}$, (i.e., roughly equimolar amount of lactones (−)-**9** and (−)-**10**). Both MO21 and MO23 each gave a mixture of lactones with the 3-oxa lactone in good *ee*, but with racemic 2-oxa lactone. Overall, the combined results illustrate an impressive range of selectivities all garnered from a single DNA sample, the extremes of which might not have been accessible using the directed evolution of a single enzyme, and which might now be employed to further develop some of the more interesting activities.

Discussion

Sequence–activity relationships

The results of the biotransformations above were considered in conjunction with the grouping of *R. jostii* RHA1 BVMOs derived from the phylogenetic tree in Figure 1. In addition to groups I–V, previously defined on the basis of the bootstrap analysis, MO21 and MO23 were treated as a group intermedi-

Table 4. Analysis of residual ketone from biotransformations of **6** by strains of *E. coli* expressing each of 13 BVMOs from *R. jostii* RHA1.

Biocatalyst	Conversion [%]	Recovered ketone	*ee*[a] (**6**) [%]	*E*[b] (**6**)
MO3	59	(1*S*,5*R*)-**6**	82	9
MO4	58	(1*R*,5*S*)-**6**	31	2
MO9	35	(1*S*,5*R*)-**6**	53	156
MO10	97	(1*R*,5*S*)-**6**	>99	3
MO11	41	(1*S*,5*R*)-**6**	17	2
MO14	36	(1*S*,5*R*)-**6**	63	25
MO15	19	(1*S*,5*R*)-**6**	21	18
MO16	43	(1*R*,5*S*)-**6**	45	6
MO18	98	(1*S*,5*R*)-**6**	87	2
MO20	75	(1*R*,5*S*)-**6**	24	1
MO21	96	(1*S*,5*R*)-**6**	99	3
MO22	51	(1*S*,5*R*)-**6**	66	9
$CHMO_{9871}$	41	(1*R*,5*S*)-**6**	10	2

[a] The margins of error in the determinations of *ee* are of the order of 1% *ee* according to data obtained for the standard racemic compound. [b] *E* for the MO14-catalysed biotransformation was generally calculated from the equation in refs. [37] and [38].

Table 5. Analysis of lactone products from biotransformations of **6** by strains of *E. coli* expressing each of 13 BVMOs from *R. jostii* RHA1.

Biocatalyst	Product lactones	*ee*[a] [%] (yield [%]) **9**	**10**
MO3	(1*S*,5*R*)-**10**	traces of **9**	47 (57)
MO4	(1*R*,5*S*)-**10**	traces of **9**	22 (54)
MO9	(1*S*,5*R*)-**9** and (1*S*,5*R*)-**10**	99 (18)	72 (17)
MO10	(1*R*,5*S*)-**9** and (1*S*,5*R*)-**10**	>99 (50)	95 (47)
MO11	(1*S*,5*R*)-**10**	traces of **9**	18 (41)
MO14	(1*S*,5*R*)-**10**	–	86 (36)
MO15	(1*S*,5*R*)-**9** and (1*S*,5*R*)-**10**	>99 (8)	64 (11)
MO16	(1*R*,5*S*)-**9** and (1*S*,5*R*)-**10**	99 (31)	83 (12)
MO18	(1*R*,5*S*)-**9** and (1*S*,5*R*)-**10**	97 (45)	87 (53)
MO20	(1*R*,5*S*)-**10**	traces of **9**	5 (75)
MO21	(1*S*,5*R*)-**9** and (1*R*,5*S*)-**10**	96 (30)	27 (66)
MO22	(1*S*,5*R*)-**10**	traces of **9**	53 (46)
$CHMO_{9871}$	(1*R*,5*S*)-**9** and (1*S*,5*R*)-**10**	98 (17)	87 (24)

[a] The margins of error in the determinations of *ee* are of the order of 2% *ee* for lactone **9** and 1% *ee* for lactone **10** according to data obtained for the standard racemic compounds.

ate between groups I and II, and enzyme MO22 was treated as a divergent enzyme.

Group I enzymes (MO3, MO4, MO11 and MO20) each converted all of the test substrates. MO14, although a group II enzyme by overall sequence, also displays this wide spectrum of activity. The other members of group II, MO9 and MO15 transformed a range of substrates that did not include either cyclohexanone or cycloheptanone. MO21 and MO23 did not convert cycloheptanone, but exhibited a preference for C_6 and C_5 cyclic ketones over octan-2-one, in common with $BVMO_{mekA}$,[16] with which these enzymes cluster in the phylogenetic tree in Figure 1. MO16, which clustered with $BVMO_{KT2440}$, an enzyme that had a high specificity toward short-chain aliphatic ketones,[17] displayed the best activity of all the *R. jostii* MOs for the aliphatic ketone substrate **7**. $CHMO_{9871}$ displayed behaviour consistent with the literature. Group IV enzymes MO10 and MO18 both displayed narrow substrate specificities. Even at this level of analysis, these results indicate that, with the notable exception of MO14, there is a pronounced sequence–activity relationship among the enzymes in groups I and II in this study.

Turning to the enantioselectivity of the enzymes, group I enzymes MO3, MO4, MO11 and MO20 catalysed poorly enantioselective transformations of **5.** This was also true of enzymes 21 and 23. Group II enzymes MO9 and MO15 exhibited *R*-selectivity. Once again, MO14 displayed "group I behaviour" in catalysing the transformation with a low *E* value. This group-specific behaviour extended to transformations of the racemic bicyclic ketone **6.** Group I enzymes MO3, MO4, MO11 and MO20 formed the 2-oxalactone **10** only. Group II enzymes MO9 and MO15 produce both **10** and 3-oxalactone **9**, each in high *ee*, from the same substrate enantiomer. MO21 and MO23 produce a mixture of **10** and **9**, the former with poor *ee*. MO14 is again anomalous, producing the 2-oxalactone only, in the mode of group I enzymes, yet utilizing predominantly one substrate enantiomer, as observed with group II. Despite low sequence homology with $CHMO_{9871}$ overall, group IV enzymes MO10 and MO18 display the classical enantiodivergent group III behaviour with ketone **6.**

The catalytic behaviour of enzymes within the better-defined groups was therefore shown to correlate well with sequence. The major exception throughout the analysis was MO14, notable in that it displayed largely group I behaviour, even though its overall sequence places it within group II with MO9 and MO15. This led us to examine the MO14 sequence for distinctive regions of amino acid sequence that were identical to the group I enzymes and yet distinct from group II enzymes. These sequences would presumably be short, because they do not have a major influence on alignment programs such as ClustalW2. One example of a region of sequence that matched these criteria was F^{208}QR<u>T</u>PN^{213} in MO14, shared by group I enzymes such as F^{211}QR<u>T</u>PN^{216} in MO3 (Figure 4, left). The corresponding sequence in group II enzymes featured a serine in place of the threonine in either MO9 (F^{206}QR<u>S</u>PN^{211}) or MO15 (F^{215}QR<u>S</u>AN^{220}). In the three-dimensional structure of PAMO,[9] the threonine residue found in this sequence in the group I enzymes and CPMO, which is replaced by serine in group 2 enzymes is adjacent to the arginine residue that has been mooted as one of the determinants of NADP specificity in PAMO[9] and is clearly seen at the lip of the entrance to the active site at the surface of that enzyme. Group I catalysts with threonine in this position display "CPMO-type" behaviour with ketone **6** as previously described by Mihovilovic and co-workers[23] and were, on the whole, more active than group II enzymes, even when levels of soluble expression were comparable (see SDS-PAGE gels in the Supporting Information), however, confirmation that this motif is responsible for differences in catalytic performance must await a detailed kinetic study of the relevant purified enzymes.

A second short region of sequence shared by group I enzymes and MO14 was P^{431}<u>Q</u>SP^{434} (MO14), also found, for exam-

MO10	LDVVVRSPHWLVPEK	357	MO10	ITAGPNSAPNHGAGH	557
MO18	LSIYQRSPQWVAPFE	362	MO18	MLGGPNSFPGSGS-F	561
HAPMO	LKVFARTTNWLLPTP	348	HAPMO	CMYGPNTGLVVYSTV	549
MO11	ITI**FQRTPN**LALPMR	226	MO11	FVYG**PQSP**AG-FCNG	449
MO20	VTV**FQRTPN**LAIPMQ	229	MO20	FLYG**PQSP**SG-FCNG	452
CPMO	VTVYQRTPNLALPMH	230	CPMO	FGYGPQSPAG-FCNG	453
MO3	LTV**FQRTPN**TALPMN	222	MO3	YVYG**PQSP**NA-FCNG	446
MO4	LTV**FQRTPN**ISLPMQ	227	MO4	FVYG**PQSP**AA-FANG	452
MO9	VFV**FQRSPN**YSIPAG	217	MO9	ILAG**AGSP**SV-LANM	437
MO15	LYV**FQRSAN**YSVPAG	226	MO15	VVTG**PGSP**SV-LANM	446
MO14	LVV**FQRTPN**FATPLG	219	MO14	LITG**PQSP**SV-LYNM	440
PAMO	LFVFQRTPHFAVPAR	226	PAMO	FIAGPGSPSA-LSNM	446
CHMO	LTVFQRSAQYSVPIG	216	CHMO	MVLGPNGP---FTNL	435
MO21	LKVFIRTPQYALPMK	227	MO21	TTGAPLAPSAALCNM	450
MO23	LKVFIRTPQYALPMK	227	MO23	TTGAPLAPSAALCNM	450
MO16	VTMLQRSPTYIISMP	221	MO16	FVIG-----YTNASW	407
MO22	LPYMPFPATWPQFVP	244	MO22	MRRGGGYYLNVGCSD	467

Figure 4. Short regions of amino acid sequence in BVMOs from *R. jostii* RHA1. Left: FQRTPN in group I enzymes and MO14 and FQRS(P/A)N for group II. Right: PQSP in group I and MO14, and (P/A)GSP in group II sequences.

ple, in MO3 as P^{437}QSP^{440} (Figure 4, right). The glutamine in this short sequence is typically replaced by a glycine in the sequence A^{428}GSP^{431} found in group II enzymes such as MO9 and is also seen in PAMO. This quartet of amino acids is adjacent to the "bulge" identified in PAMO that was thought to be important in substrate acceptance and stereoselectivity. Removal of this bulge resulted in a PAMO variant of increased substrate range.[33] MO10, MO18 and $CHMO_{9871}$, whilst of low overall sequence identity, share an asparagine residue in the equivalent position, as well as common enantioselectivity with respect to substrate **6**, as do each of the "CHMO-type" group of enzymes described previously[19,23] and featured in the tree in Figure 1. Amino acids close to this sequence had already been highlighted by Mihovilovic and co-workers, who suggested that the enantioselectivity of enzymes in either "CHMO-type" or "CPMO-type" groups could be at least partially dependent on the occurrence of a phenylalanine (CPMO) or leucine ($CHMO_{9871}$) at position 432 ($CHMO_{9871}$ numbering), located immediately downstream of the PQSP and PGSP quartets in *R. jostii* RHA1 enzymes (Figure 4). Changes in the enantioselectivity of $CHMO_{9871}$ were observed upon substituting Phe432 to a serine in this enzyme.[34] Interestingly, whilst MO9, MO15 and MO14 share the same sequence in the "bulge" region and also a leucine in a position equivalent to Phe432 of $CHMO_{9871}$, they display different stereochemical behaviour with respect to both substrates **5** and **6**. Whilst it has been shown that the exquisite and distinct catalytic and enantioselective properties of BVMOs are most likely to be dependent on interactions that are dependent on more than one or two amino acids, the identification of short regions of amino acid sequence that correlate with subgroup-specific behaviour could prove helpful in assigning substrate specificity and enantioselective properties from sequence alone in some genomic targets.

Conclusions

Activity profiling and sequence analyses of the BVMOs from *R. jostii* RHA1 have revealed that the diversity of sequence amongst flavoenzymes that are capable of catalysing the Baeyer–Villiger reaction is extremely broad even within a single genome, and that a variety of mechanisms of substrate recognition and molecular determination of enantioselectivity might operate within this enzyme family as a whole. Some of these characteristics may increasingly be detected from genomic sequence alone as the amount of data from both random mutagenesis and genome mining experiments increases. From the point of view of preparative chemistry, it is encouraging that a wealth of selectivities exists that may be accessed comparatively easily and that each new enzyme of distinct selectivity presents a valuable starting point for optimisation through laboratory-based evolution for the reaction of choice.

Experimental Section

Gene cloning: The target genes were amplified by using the genomic DNA of *R. jostii* RHA1 as a template. PCR primers (detailed in the Supporting Information) were obtained from MWG Biotech (Ebersberg, Germany). The PCR products were cloned into the pET-YSBLIC-3C vector by using a ligation-independent cloning method described in ref. [13]. The correct sequence of all plasmids was confirmed by DNA sequencing, which was carried out by MWG Biotech (London, UK). Photographs showing agarose gels of restriction digests of the relevant plasmids are given in the Supporting Information.

Gene expression: *E. coli* Rosetta 2 (DE3) pLysS was used as the expression strain for creating the recombinant biocatalysts. Expression tests were routinely conducted in 5 mL cultures in LB broth that had been inoculated with a 10% inoculum from an overnight culture of the relevant strain. Cells were grown at 37 °C until an OD_{600} of 0.6 had been reached, at which point gene expression was induced by the addition of isopropyl-β-D-thiogalactopyranoside (1 mM). The cells were then grown at 20 °C for 16 h with shaking at 180 rpm. In each case, the harvested cell pellet was resuspended in Tris/HCl buffer (20 mM, pH 8.0) containing NaCl (500 mM). The cell suspensions were gently sonicated on ice, and the soluble and insoluble fractions of the cell lysate were analysed by SDS-PAGE. Photographs of gels showing the overexpression of soluble targets are provided in the Supporting Information.

Whole-cell biotransformations: All of the whole-cell biotransformation tests were carried out with growing cells according to the overexpression protocol above. The substrates were dissolved in neat ethanol and added to cell culture (1 mL) 3 h after induction to give a final concentration of 1% (*v*/*v*) ethanol in the medium. The final substrate concentrations were 17 mM for ketone **1**,

14 mM for ketone **2**, 12 mM for ketone **3**, 11 mM for ketone **4**, 12 mM for ketone **5**, 13 mM for ketone **6** and 8 mM for ketone **7**. Reaction mixtures were extracted from the LB medium with ethyl acetate and analysed by using an Agilent Technologies 6890N gas chromatograph equipped with an HP-5 column under the conditions described below. Substrates **1** to **7** and their corresponding lactones/esters had been purchased from Sigma–Aldrich and were used as standards. Oxocan-2-one (the lactone derived from cycloheptanone **4**) was identified by using the biotransformation of **4** catalysed by CHMO from *Acinetobacter calcoaceticus* NCIMB 9871.[21]

GC analysis

Standard GC: For standard GC analysis, an Agilent HP-6890 gas chromatograph was employed, fitted with an HP-5 column (30 m × 0.32 mm × 0.25 μm). Helium was used as the carrier gas at a pressure of 83 kPa. The injector temperature was 250 °C, and the detector temperature was 320 °C. The gradient programme used for analysis of biotransformation reactions with substrates **1**, **2** and **4** was 50 to 100 °C at 10 °C min^{-1} then 100 to 250 °C at 30 °C min^{-1}. The retention times for substrates and products were **1**: 1.94 min, γ-butyrolactone: 4.04 min, **2**: 2.53 min, δ-valerolactone: 5.73 min, **4**: 4.98 min, oxocan-2-one: 7.75 min. The gradient programme used for analysis of biotransformation reactions with substrates **3**, **5**, **6** and **7** was 50 to 250 °C at 10 °C min^{-1}. The retention times for substrates and products were **3**: 3.44 min, ε-caprolactone: 7.03 min, **5**: 3.00 min, **8**: 6.26 min, **6**: 4.04 min, **9** + **10**: 7.70 min, **7**: 4.69 min, hexyl acetate, 4.90 min.

Chiral GC: For chiral GC analysis both a BGB-173 column and a BGB-175 column (each 30 m × 0.25 mm × 0.25 μm, BGB Analytik) were employed. For all analyses, helium was used as the carrier gas at a pressure of 83 kPa, the injector temperature was 250 °C, and the detector temperature was 320 °C. Enantiomers of substrate **5** were resolved on the BGB-175 column with a temperature gradient of 70 to 82 °C at 0.5 °C min^{-1}. Enantiomer retention times were (*S*)-**5**: 20.65 min, (*R*)-**5**: 21.35 min. Enantiomers of lactone **8** were resolved on the BGB-173 column with a gradient of 100 to 140 °C at 2 °C min^{-1}. The enantiomer retention times were (*R*)-**8**: 18.44 min, (*S*)-**8**: 18.76 min. Enantiomers of substrate **6** were resolved on the BGB-175 column with a gradient of 100 to 127 °C at 2 °C min^{-1}. Enantiomer retention times were (1*R*,5*S*)-(+)-**6**: 11.46 min, (1*S*, 5*R*)-(−)-**6**: 12.26 min. Enantiomers of lactones **9** and **10** were resolved on the BGB-173 column with a gradient of 90 to 134 °C at 1 °C min^{-1}. Enantiomer retention times were (1*R*,5*S*)-(−)-**9**: 36.70 min, (1*S*,5*R*)-(+)-**9**): 37.01 min, (1*S*,5*R*)-(−)-**10**: 41.82 min, (1*R*,5*S*)-(+)-**10**: 42.40 min.

Phylogenetic analyses: Sequences used for the phylogenetic analysis were aligned by using CLUSTALW (default settings).[22] Phylogenetic analyses were performed by using the alignment and the PHYLIP package, version 3.[35] Phylogenetic trees were calculated based on protein maximum likelihood by using PROML. The best tree was obtained from 21 jumbles of the input alignment. For bootstrap analyses, 100 datasets were generated by using SEQBOOT, and the best tree of each dataset was calculated by using PROML and seven jumbles. The final consensus tree was calculated by using CONSENSE. Trees were plotted by using TREEVIEW.[36]

Acknowledgements

We would like to thank the Centre of Excellence for Biocatalysis, Biotransformations and Biomanufacture (CoEBio3) for funding a Ph.D. studentship to C.S. We would also like to thank Prof. Dr. Marko Mihovilovic (Technical University, Vienna) for the gift of plasmid pMMO4, containing the gene encoding $CHMO_{9871}$. L.D.E. was supported through a Natural Sciences and Engineering Research Council (NSERC) of Canada Discovery Grant.

Keywords: Baeyer–Villiger reaction · enzyme catalysis · ketones · oxidoreductases · stereoselectivity

[1] N. A. Donoghue, D. B. Norris, P. W. Trudgill, *Eur. J. Biochem.* **1976**, *63*, 175–192.
[2] G. R. Krow, *Org. React.* **1993**, *43*, 251–798.
[3] A. Watanabe, T, Uchida, K. Ito, T. Katsuki, *Tetrahedron Lett.* **2002**, *43*, 4481–4485.
[4] N. M. Kamerbeek, D. B. Janssen, W. J. H. van Berkel, M. W. Fraaije, *Adv. Synth. Catal.* **2003**, *345*, 667–678.
[5] M. D. Mihovilovic, *Curr. Org. Chem.* **2006**, *10*, 1265–1287.
[6] M. W. Fraaije, J. Wu, D. P. H. M. Heuts, E. W. van Hellemond, J. H. Lutje Spelberg, D. B. Janssen, *Appl. Microbiol. Biotechnol.* **2005**, *66*, 393–400.
[7] M. W. Fraaije, N. M. Kamerbeek, W. J. H. van Berkel, D. B. Janssen, *FEBS Lett.* **2002**, *518*, 43–47.
[8] W. J. H. van Berkel, N. M. Kamerbeek, M. W. Fraaije, *J. Biotechnol.* **2006**, *124*, 670–689.
[9] E. Malito, A. Alfieri, M. W. Fraaije, A. Mattevi, *Proc. Natl. Acad. Sci. USA* **2004**, *101*, 13157–13162.
[10] M. T. Reetz, B. Brunner, T. Schneider, F. Schulz, C. M. Clouthier, M. M. Kayser, *Angew. Chem.* **2004**, *116*, 4167–4170; *Angew. Chem. Int. Ed.* **2004**, *43*, 4075–4078.
[11] C. M. Clouthier, M. M. Kayser, M. T. Reetz, *J. Org. Chem.* **2006**, *71*, 8431–8437.
[12] D. E. Torres Pazmiño, R. Snajdrova, D. V. Rial, M. D. Mihovilovic, M. W. Fraaije, *Adv. Synth. Catal.* **2007**, *349*, 1361–1368.
[13] D. Bonsor, S. F. Butz, J. Solomons, S. Grant, I. J. S. Fairlamb, M. J. Fogg, G. Grogan, *Org. Biomol. Chem.* **2006**, *4*, 1252–1260.
[14] A. Kirschner, U. T. Bornscheuer, *Angew. Chem.* **2006**, *118*, 7161–7163; *Angew. Chem. Int. Ed.* **2006**, *45*, 7004–7006.
[15] A. Kirschner, J. Altenbuchner, U. T. Bornscheuer, *Appl. Microbiol. Biotechnol.* **2007**, *73*, 1065–1072.
[16] A. Völker, A. Kirschner, U. T. Bornscheuer, J. Altenbuchner, *Appl. Microbiol. Biotechnol.* **2008**, *77*, 1251–1260.
[17] J. Rehdorf, A. Kirschner, U. T. Bornscheuer, *Biotechnol. Lett.* **2007**, *29*, 1393–1398.
[18] D. V. Rial, D. Bianchi, P. Kapitanova, A. Lengar, J. van Beilen, M. D. Mihovilovic, *Eur. J. Org. Chem.* **2008**, 1203–1213.
[19] D. V. Rial, P. Cernuchova, J. B. van Beilen, M. D. Mihovilovic, *J. Mol. Catal. B* **2008**, *50*, 61–68.
[20] M. P. McLeod, R. L. Warren, W. W. L. Hsiao, N. Araki, M. Myhre, C. Fernandes, D. Miyazawa, W. Wong, A. L. Lillquist, D. Wang, M. Dosanjh, H. Hara, A. Petrescu, R. D. Morin, G. Yang, J. M. Stott, J. E. Schein, H. Shin, S. Smailus, A. S. Siddiqui, M. A. Marra, S. J. M. Jones, R. Holt, F. S. L. Brinkman, K. Miyauchi, M. Fukuda, J. E. Davies, W. W. Mohn, L. D. Eltis, *Proc. Natl. Acad. Sci. USA* **2006**, *103*, 15582–15587.
[21] N. M. Kamerbeek, M. J. H. Moonen, J. G. M. van der Ven, W. J. H. van Berkel, M. W. Fraaije, D. B. Janssen, *Eur. J. Biochem.* **2001**, *268*, 2547–2557.
[22] M. A. Larkin, G. Blackshields, N. P. Brown, R. Chenna, P. A. McGettigan, H. McWilliam, F. Valentin, I. M. Wallace, A. Wilm, R. Lopez, J. D. Thompson, T. J. Gibson, D. G. Higgins, *Bioinformatics* **2007**, *23*, 2947–2948.
[23] M. D. Mihovilovic, F. Rudroff, B. Grötzl, P. Kapitan, R. Snajdrova, J. Rydz, R. Mach, *Angew. Chem.* **2005**, *117*, 3675–3679; *Angew. Chem. Int. Ed.* **2005**, *44*, 3609–3613.
[24] M. W. Fraaije, N. M. Kamerbeek, A. J. Heidekamp, R. Fortin, D. B. Janssen, *J. Biol. Chem.* **2004**, *279*, 3354–3360.
[25] P. Černuchová, M. D. Mihovilovic, *Org. Biomol. Chem.* **2007**, *5*, 1715–1719.
[26] R. Snajdrova, I. Braun, T. Bach, K. Mereiter, M. D. Mihovilovic, *J. Org. Chem.* **2007**, *72*, 9597–9603.
[27] V. Alphand, A. Archelas, R. Furstoss, *Tetrahedron Lett.* **1989**, *30*, 3663–3664.

[28] R. Gagnon, G. Grogan, M. S. Levitt, S. M. Roberts, P. W. H. Wan, A. J. Willetts, *J. Chem. Soc. Perkin Trans. 1* **1994**, 2537–2544.
[29] M. M. Kayser, G. Chen, J. D. Stewart, *J. Org. Chem.* **1998**, *63*, 7103–7106.
[30] J. D. Stewart, *Curr. Org. Chem.* **1998**, *2*, 195–216.
[31] H. Iwaki, S. Wang, S. Grosse, H. Bergeron, A. Nagahashi, J. Lertvorachon, J. Yang, Y. Konishi, Y. Hasegawa, P. C. K. Lau, *Appl. Environ. Microbiol.* **2006**, *72*, 2707–2720.
[32] R. Snajdrova, G. Grogan, M. D. Mihovilovic, *Bioorg. Med. Chem. Lett.* **2006**, *16*, 4813–4817.
[33] M. Bocola, F. Schulz, F. Leca, A. Vogel, M. W. Fraaije, M. T. Reetz, *Adv. Synth. Catal.* **2005**, *347*, 979–986.
[34] C. M. Clouthier, M. M. Kayser, *Tetrahedron: Asymmetry* **2006**, *17*, 2649–2653.
[35] J. Felsenstein, *Cladistics* **1989**, *5*, 164–166.
[36] R. D. M. Page, *Comp. Appl. Biosci.* **1996**, *12*, 357–358.
[37] C.-S. Chen, Y. Fujimoto, G. Girdaukas, C. J. Sih, *J. Am. Chem. Soc.* **1982**, *104*, 7294–7299.
[38] J. L. L. Rakels, A. J. J. Straathof, J. J. Heijnen, *Enzyme Microb. Technol.* **1993**, *15*, 1051–1056.

Received: January 7, 2009
Published online on April 9, 2009

